Civil Engineering Infrastructures Journal xx,xx

DOI: 10.22059/ceij.2025.392268.2275

A novel and efficient simulation method of structural reliability for Gaussian distributed variables by the introduction of a truncated probability density function

Roudak, M.A.[1*], Farahani, M.[2], Badiezadeh, S.[2], Amiri Beirami, M.[2], Kiashemshaki, S.[2], Karamloo, M.[3]

[1]Assistant Professor, Department of Civil Engineering, Faculty of Engineering, Alzahra University, Tehran, Iran.
[2]Graduate Student, Department of Civil Engineering, Faculty of Engineering, Alzahra University, Tehran, Iran.
[3]PhD, Department of Civil Engineering, Shahid Rajaee Teacher Training University, Lavizan, Tehran, Iran.

Received: 17/03/2025

Revised: 26/08/2025

Accepted: 03/10/2025

ABSTRACT

In structural reliability analysis, finding an effective way to estimate the probability of failure of structures, is one of the most fundamental challenges. Monte Carlo simulation is recognized as a common method for computing the probability of failure among the various existing approaches. However, its inefficiency is still a significant drawback. Since a large number of samples is required to estimate the probability of failure accurately, the Monte Carlo simulation is a time-consuming process. In this paper, a new method is proposed to improve the efficiency of the Monte Carlo simulation. This is carried out by reducing the number of required samples. The basic concept of the presented method is to generate a smaller number of samples, mostly concentrated on the failure region. To accomplish this goal, a specific distance from the mean of the variables is eliminated from the sample generation space. In fact, the samples are

* Corresponding author E-mail: a.roudak@alzahra.ac.ir

generated based on a truncated joint probability density function. This leads to a significant reduction in the number of generated samples, enhancing the efficiency of the estimation. The accuracy and efficiency of the presented method are validated using various examples.

Keywords: *Monte Carlo simulation; Probability of failure; Truncated joint probability density function; Sampling approach*

1. Introduction

Structural reliability analysis examines how uncertainty could influence the performance of a structure (Meng et al., 2024a; Meng et al., 2023a). It actually intends to assess the probability of failure regarding a given behavior in structures. This requires evaluating a limit state function (LSF) for a specified vector **X**, which includes *n* random variables. *f* defines the joint probability density function, and ultimately, the probability of failure is denoted by P_f with

$$P_f = \int_{g(\mathbf{X})<0} f_X(\mathbf{X}) d(\mathbf{X}) \quad (1)$$

It is important to note that in most engineering problems, the LSF is usually unclear and its estimation would be difficult. Thus, approximation and simulation methods have been suggested as possible solutions for this matter (Roudak et al., 2023; Pokusiński and Kamiński, 2023). The first-order reliability method (FORM) and the second-order reliability method (SORM), known as approximation methods, are frequently used in the analysis of structural reliability problems due to their efficiency and accuracy (Kumar et al., 2024). These methods simplify the analytical expression using a first- or second-order Taylor expansion. According to FORM, Hasofer and Lind provided an iterative approach for calculating the reliability index

β (Hasofer and Lind, 1974; Shayanfar et al., 2018). In this method, LSF is approximated at the design point, which is a point on the limit state surface with the closest distance to the origin of the standard normal coordinate system. This distance is actually equal to the aforementioned reliability index β. Using chaos control, Yang proposed the stability transformation method (STM) (Yang, 2010). Using a second-order polynomial as the reliability function, Keshtegar and Miri proposed a reliability algorithm (Keshtegar and Miri, 2013). Kaminski and Solecka used the perturbation-based stochastic finite element method for optimization of the structures (Kamiński and Solecka, 2013). Dang et al. carried out the Bayesian approach to structural reliability (Dang et al., 2022). By means of confidence interval squeezing, Chen et al. proposed an adaptive reliability method (Chen et al., 2022). Approximation methods could be generally appropriate choices. Nevertheless, they require differentiable explicit LSFs, and this condition cannot be fulfilled in some cases.

Monte Carlo simulation (MCS) is known as a fundamental simulation method, which has a wide application in different engineering problems. In MCS, the probability of failure is estimated using random samples that are generated through a repetitive numerical process (Peng et al., 2017b; Roudak et al., 2024). MCS is accurate in comparison with other reliability methods. Moreover, it is unaffected by complex LSF. However, it can be inefficient for practical reliability problems with low probability of failures. In fact, this method requires a large number of samples to be accurate, implying that the computation time can be high. To solve this problem, researchers have proposed various algorithms to enhance the behavior of MCS (Yang et al., 2025). Importance sampling is one of these methods, which involves sampling by a different distribution instead of the original distribution. The aforementioned alternative distribution is specifically designed to assign greater importance to those regions of the sample space that are near the failure region. Another popular method is Latin Hypercube Sampling (LHS). This method improves the efficiency of MCS by dividing the cumulative

density function (CDF) of variables into equal intervals. This guarantees thorough coverage of the whole sample space and results in a more effective estimation of the probability of failure. Many other efforts were also made in this regard, effectively enhancing the MCS method. The Directional sampling method (Au and Beck, 2001), Line sampling method (Chen and Yang, 2019), Subset simulation method (Xiao et al., 2020), Direct probability integral method (Hong et al., 2021; Zhang and Xu, 2021b; Zhang and Xu, 2021a), M5 model tree (Keshtegar and Kisi, 2017), and hybrid enhanced MCS (HEMCS) (Luo et al., 2022) are other significant approaches (Meng et al., 2023b; Meng et al., 2024b). Adaptive importance sampling (AIS) changes the sampling density function (SDF) sample by sample to ensure efficient sampling at each step (Xiao et al., 2023). Zhu et al. presented a probabilistic model for locating the design point (Zhu et al., 2020). Hao et al. carried out a sequential single-loop reliability optimization and confidence analysis method (Hao et al., 2022). Yeh presented a self-adaptive simulation-based approach (Yeh, 2022). By means of machine learning, Luo et al. promoted MCS (Luo et al., 2022). Jafari-Asl et al. improved directional simulation by the Harris Hawks optimization method (Jafari-Asl et al., 2022). Lu et al. applied both the kriging proxy model and the KNN algorithm to promote the accuracy and efficiency in complex structures analysis (Lu et al., 2022). Afshari et al. proposed the machine learning-based reliability and the application of artificial neural network methods (Afshari et al., 2022). Sun et al. provided machine learning for structural design and prediction of structural performance (Sun et al., 2021). Guo et al. proposed an active learning strategy to get accurate probabilistic fracture assessment results by a few samples (Guo et al., 2022). Wang et al. applied machine learning in reliability analysis of functionally graded frame structures under static loading (Wang et al., 2020). In recent years, machine learning-based methods have found their superiority over classical methods. Roy and Chakraborty, applied support vector machine in structural reliability (Roy and Chakraborty, 2023). Adaptive artificial neural networks are combined with structural reliability analysis in

many researches (de Santana Gomes, 2019). Cheng and Lu carried out a reliability research based on ensemble learning of surrogate models (Cheng and Lu, 2020).

Du and Hu proposed FORM with truncated random variables (Du and hu, 2012). Xiao et al. reached a surrogate-model-based reliability method for structural systems with dependent truncated random variables (Xiao et al., 2017). Qin et al. proposed an improved active kriging method based on truncated importance sampling for reliability analysis (Qin et al., 2022). Cheng et al. presented a time-dependent reliability analysis of planar mechanisms considering truncated random variables (Cheng et al., 2024). Zhou et al. represented a structural reliability analysis based on the probability density evolution method and stepwise truncated variance reduction (Zhou et al., 2024). Pokusinski and Kaminski carried out numerical convergence and error analysis for the truncated iterative generalized stochastic perturbation-based finite element method (Pokusiński and Kamiński, 2023).

Despite the above-mentioned enhancements, high-dimensional nonlinear problems still suffer from expensive repeated simulations, therefore it is computationally difficult to estimate the probability of failure accurately (Zhou et al., 2020; Luo et al., 2022).

The current research presents a modified method based on MCS, which can reduce the computational time while keeping high accuracy. Traditional MCS methods are well known for their reliability and simplicity, but they often require very large computational effort, especially for large-scale or complex reliability problems. The proposed algorithm solves these issues by using an improved sampling strategy with a more efficient calculation process. This makes the method estimate the probability of failure faster, with much lower computational cost. In addition, the algorithm keeps the generality and flexibility of the standard MCS approach, which makes it suitable for many types of structural and reliability analysis. To verify its effectiveness, the algorithm has been tested on several mathematical problems and

engineering case studies, and the results show consistent improvements in both accuracy and efficiency compared with existing simulation methods.

2. Proposed method

As mentioned before, MCS is used as a simulation method in reliability analysis based on generating random samples for computing the probability of failure. The generated samples accumulate around the mean of the variables, which are typically located in the safe region. Therefore, generating a large number of samples is required to reach the failure region. This paper presents a new method that increases efficiency while preserving accuracy. In order to achieve this goal, it is essential to increase the concentration of generated samples in the failure region to avoid the large time consumption associated with producing a large number of samples. This approach enables a more efficient estimation of the probability of failure. In this method, the sample space is limited to a section near the failure region, resulting in more samples being located in this region. Thus, computing the probability of failure is possible by generating fewer samples.

In the following subsections, the proposed method is presented with a more detailed description. In section 2.1, the process of truncating the Joint Probability Density Function (JPDF) is defined. JPDF defines the probabilistic behavior of a set of continuous random variables, jointly represented as a continuous random vector. In this paper, JPDF is the *n*-dimensional Gaussian distribution where *n* is the number of random variables. Section 2.2 describes the sampling approach. In section 2.3, the volume under the truncated JPDF is computed, and using this volume, the probability of failure is estimated in section 2.4.

2.1. Determination of the truncated region

This section discusses how to reduce the number of samples in order to estimate the probability of failure more efficiently. The concept of this method is based on reducing the concentration of samples in the safe region by preserving the nature of the corresponding distribution. For

this purpose, a part of the JPDF around the mean of the random variables is truncated, so that no samples are generated in this region. The decision on how much of this area should be removed will be further discussed and examined. Fig. 1 indicates the truncated JPDF and the resulting generated samples. As shown, eliminating the certain middle part of the JPDF prevents the generation of samples around the mean of the JPDF.

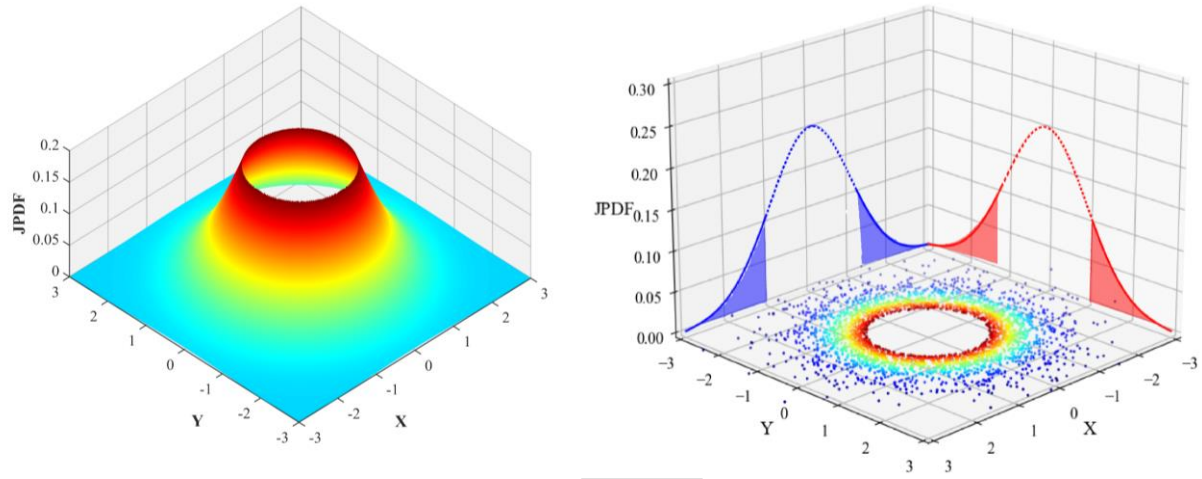

Fig. 1. The 3D illustration of truncated JPDF and the resulting sampling

In order to truncate this segment of the JPDF, a circle of radius R centered at the mean of the random variables is created, and the samples are generated outside of this circle. R is determined as follows:

In the first step, a certain number of samples are generated uniformly in the whole area, and then the LSF is evaluated at these samples. Next, all samples located in the failure region are determined, and their distance from the origin is measured. Subsequently, the sample in the failure region with the shortest distance d to the origin is selected. A certain percentage of this distance is considered as the radius R that determines the truncated region of JPDF. This percentage, represented by a, should be chosen in a way that almost no part of the failure region is eliminated

$$R = a\|d\| \tag{2}$$

Based on trial and error, it appears that setting the value of a in the range of 0.7 to 0.9 implies that the entire failure region is almost covered.

2.2. Sampling approach

The procedure for generating samples and determining the region, in which the samples should be produced, is presented in this section. As mentioned, the goal is to remove a circular region with a radius R from the mean of the variables and generate the samples outside this region. Thus, no samples are generated within this middle circular region. As a result, the failure region could be reached by generating fewer samples. The following equation presents the sampling approach

$$S_j = \boldsymbol{\lambda} \times \left[\Phi^{-1} \left(\Phi(R) + \alpha (1 - \Phi(R)) \right) \right] \quad (3)$$

where S_j is the generated sample, Φ is the CDF of the standard normal distribution, α is a random number between 0 and 1, and $\boldsymbol{\lambda}$ is used as a random unit vector. This vector causes the random variables to be distributed in the whole desired sample space. In fact, the unit vector $\boldsymbol{\lambda}$ clarifies the direction of the sample, which is to be generated. The scalar multiplied by $\boldsymbol{\lambda}$ lengthens or shortens the direction vector and therefore adjusts the distance of the sample from the origin in the direction of $\boldsymbol{\lambda}$. This scalar is obtained based on the standard normal distribution, i.e. the distribution of random variables in U-space. $\Phi(R) + \alpha(1 - \Phi(R))$ gives a random number for CDF between $\Phi(R)$ and 1. The inverse CDF of this number returns a value larger than R.

2.3. The volume under the truncated JPDF

To evaluate the probability of failure, it is necessary to calculate the volume under the truncated JPDF. Firstly, the random variables are transformed into the standard normal coordinate system (U-space). Assuming that the random variables of the multivariate LSF are independent, the volume of the truncated or removed part is obtained from this integral equation

$$V_t = \int_{D:x_1^2+x_2^2+\cdots+x_n^2<R} (2\pi)^{\frac{-n}{2}} e^{\frac{-1}{2}(x_1^2+x_2^2+\cdots+x_n^2)} dA \tag{4}$$

By converting to polar coordinates and using the absolute value of the Jacobian, the volume is computed using the following integral

$$V_t = \int_{\theta_{n-1}=0}^{\theta_{n-1}=\pi} \cdots \int_{\theta_2=0}^{\theta_2=\pi} \int_{\theta_1=0}^{\theta_1=2\pi} \int_{r=0}^{r=R} (2\pi)^{\frac{-n}{2}} e^{\frac{-1}{2}} r^{n-1} \left[\prod_{k=2}^{n-1} \sin^{k-1}\theta_k\right] dr d\theta_1 d\theta_2 \cdots d\theta_{n-1} \tag{5}$$

with

$$\begin{aligned} 0 \le r \le R \\ 0 \le \theta_1 \le 2\pi \\ 0 \le \theta_j \le \pi \quad \text{for } j = 2 : n-1 \end{aligned} \tag{6}$$

By applying the above equation, the following integral can be obtained

$$\begin{aligned} V_t = (2\pi)^{\frac{-n}{2}} \times \left[\int_0^R e^{\frac{-1}{2}r^2} r^{n-1} dr\right] \times \left[\int_0^{2\pi} d\theta_1\right] \times \left[\int_0^{\pi} \sin\theta_2 d\theta_2\right] \\ \times \left[\int_0^{\pi} \sin^2\theta_3 d\theta_3\right] \times \cdots \times \left[\int_0^{\pi} \sin^{n-2}\theta_{n-1} d\theta_{n-1}\right] \end{aligned} \tag{7}$$

Solving the independent integrals results in

$$\begin{aligned} \int_0^R e^{\frac{-1}{2}r^2} r^{n-1} dr = \left(\sqrt{2}\right)^{n-2} \Gamma(\frac{n}{2}) \mathrm{A}\left(\frac{R^2}{2}, \frac{n}{2}\right) \\ \int_0^{\pi} \sin^m x dx = \mathrm{B}(\frac{m+1}{2}, \frac{1}{2}) \end{aligned} \tag{8}$$

with B being the beta function and described in the equation below

$$\mathrm{B}(z_1, z_2) = \frac{\Gamma(z_1)\Gamma(z_2)}{\Gamma(z_1 + z_2)} \tag{9}$$

and Γ indicating the gamma function. As a result, V_t in Eq. (7) is computed as

$$V_t = \mathrm{A}\left(\frac{R^2}{2}, \frac{n}{2}\right) \tag{10}$$

where $A\left(\frac{R^2}{2}, \frac{n}{2}\right)$ is the regularized lower incomplete gamma function, expressed as

$$\mathrm{A}(x, a) = \frac{1}{\Gamma(a)} \int_0^x t^{a-1} e^{-t} dt = \frac{2}{\Gamma(a)} \int_0^{\sqrt{x}} t^{2a-1} e^{-t^2} dt \tag{11}$$

Therefore, by knowing that the volume under the entire JPDF is equal to 1, the volume of the sampling region is obtained by

$$V_s = 1 - V_t \tag{12}$$

Since the volume of the sampling region is obtained, the probability of failure can be computed. This process will be explained in detail in the next section.

2.4. Computing the probability of failure

As mentioned before, a circle with radius R is considered under the JPDF around the mean of the variables, ensuring that no samples are generated within this region. It is crucial to consider that by employing only this truncated JPDF, a set of samples is disregarded. In fact, the deliberately eliminated samples should be considered in the total number of samples. By using the volume under the truncated region and knowing that the volume under the entire JPDF is equal to one, the total number of samples (including non-generated samples) is obtained as follows

$$N_{total} = \frac{N_s}{V_s} \tag{13}$$

where N_s indicates the number of generated samples based on the truncated JPDF. In fact, the above formulation could be interpreted in the following way, and as the response to the following question:

"How many samples should have been generated based on the complete JPDF such that N_s samples fall below the truncated JPDF?"

As the response, since N_s is proportional to the volume V_s, and the number of imaginary removed samples N_t is proportional to V_t, then N_t is equal to $N_s V_t/V_s$, and N_{total} as the sum of N_s and N_t is obtained N_s/V_s as in Eq. (13).

Therefore, the probability of failure can be computed as follows

$$P_f = \frac{N_f}{N_s} V_s \tag{14}$$

Where N_f is the number of generated samples in the failure region. Ensuring that the radius of the circle does not remove any part of the failure region implies that the excluded samples all fall within the safe region and do not affect the value of N_f.

3. Results and discussion

In this section, several examples are examined to evaluate the performance of the proposed method. The algorithm is run 10 times, and the average and standard deviation of the probability of failure, the number of samples in the failure region, and the estimation error are recorded. For each example, a table with the obtained results is provided. Results are compared to MCS, FORM, and eKNN (Peng et al., 2017b; Mooney, 1997; Roudak et al., 2024; Peng et al., 2017a) to clearly indicate the significant improvement in efficiency. Additionally, a figure corresponding to each example is presented for a better understanding of the performance of this method.

Example 1

In this example, the bivariate LSF is expressed by

$$g(X) = 0.1(x_1 - x_2)^2 - \sqrt{(x_1 + x_2)} + 2.5 \quad (15)$$

x_1 and x_2 have standard normal distributions. This function is tested with sample sizes of 500, 1000, and 5000, and the results have been recorded. The mean values and standard deviations of N_f and P_f are presented in Table 1. As shown, the proposed method provides a higher accuracy than MCS, using only 500 samples. Fig. 2 illustrates the generated samples and the limit state surface of the problem. According to this figure, generating more samples in the failure region increases the accuracy of the estimation by the same number of samples.

Table 1. Results of example 1

	Samples	Average N_f	Std N_f	Average P_f	Std P_f	P_f error (%)	CPU time
Proposed method	500	19	5.25	0.0044	9.38×10^{-4}	4.76	0.061
	1000	40	11.46	0.0043	8.12×10^{-4}	2.38	0.098
	5000	182	24.74	0.0042	3.63×10^{-4}	0.00	0.114
MCS	5000	20	3.23	0.0038	0.0011	9.52	0.129
FORM	-	-	-	0.0062	0	-	0.751
eKNN	5000	22	2.65	0.0043	5.64×10^{-4}	1.77	0.119

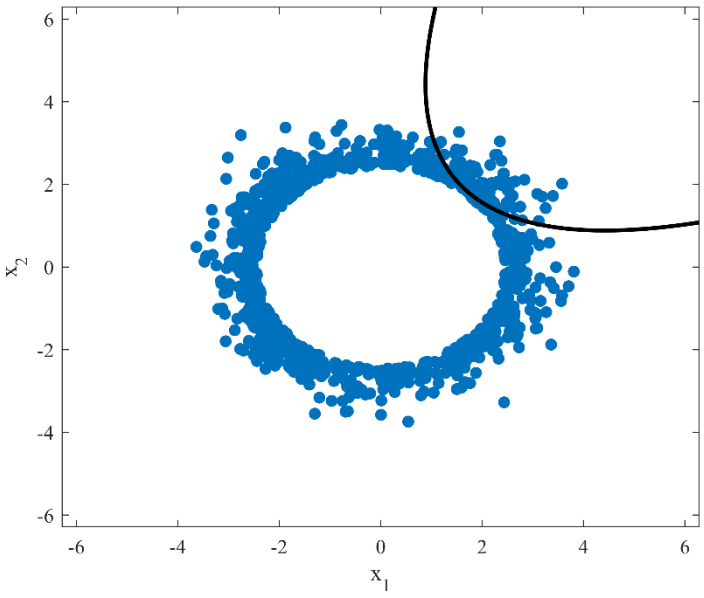

Fig. 2. The generated samples after truncating the JPDF in example 1

Example 2

In this example, the bivariate LSF is a quartic polynomial

$$g(X) = 3 - x_2 + 256x_1^4 \qquad (16)$$

The random variables are standard normally distributed. The MCS method, with a larger number of samples, estimates the probability of failure with a higher error compared to the proposed method (since most samples are generated around the mean). In Table 2, the obtained results are provided. Fig. 3 demonstrates that although the limit state surface is far from the mean of the variables, the proposed method can reach the failure region, generating only a small number of samples.

Table 2. Results of example 2

	Samples	Average N_f	STD N_f	Average P_f	Std P_f	P_f error (%)	CPU time
Proposed method	500	4	4.0222	1.58×10^{-4}	7.94×10^{-5}	5.38	0.035
	1000	10	5.831	1.62×10^{-4}	5.12×10^{-5}	2.99	0.082
	5000	48	17.5907	1.64×10^{-4}	3.19×10^{-5}	1.79	0.104
MCS	5000	0.3	0.67	3.00×10^{-4}	6.74×10^{-4}	79.64	0.108
FORM	-	-	-	0.0013	-	-	0.834
eKNN	5000	1.25	0.09	2.50×10^{-4}	3.13×10^{-5}	49.70	0.096

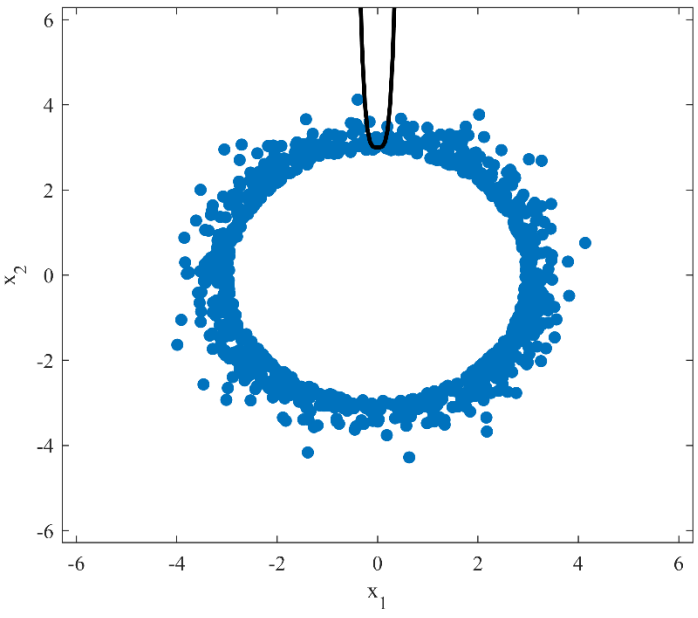

Fig. 3. The generated samples after truncating the JPDF in example 2

Example 3

In this example, the LSF is as follows

$$g(X) = -0.16(x_1 - 1)^3 - x_2 + 4 - 0.04\,cos(x_1 x_2) \quad (17)$$

Where x_1 and x_2 have standard normal distributions. Table 3 reports the obtained results using the proposed method. By generating adequate samples, this method is able to estimate the probability of failure with sufficient accuracy, whereas the MCS method requires a large number of samples to achieve accurate estimation. Fig. 4 illustrates the generated samples by the proposed method and shows how the failure region is covered by samples. Compared to the MCS, the superior efficiency in estimating the probability of failure is evident.

Table 3. Results of example 3

	Samples	Average N_f	STD N_f	Average P_f	Std P_f	P_f error (%)	CPU time
Proposed method	500	18	6.54	8.92×10^{-5}	9.84×10^{-6}	10.80	0.061
	1000	36	11.65	9.08×10^{-5}	1.86×10^{-6}	9.20	0.087
	5000	188	24.59	9.34×10^{-5}	6.12×10^{-6}	6.60	0.116
MCS	5000	0.9	0.99	1.80×10^{-4}	1.98×10^{-4}	80.0	0.112
FORM	-	-	-	2.54×10^{-5}	-	-	-
eKNN	5000	1.25	0.09	2.50×10^{-4}	3.13×10^{-5}	49.70	0.096

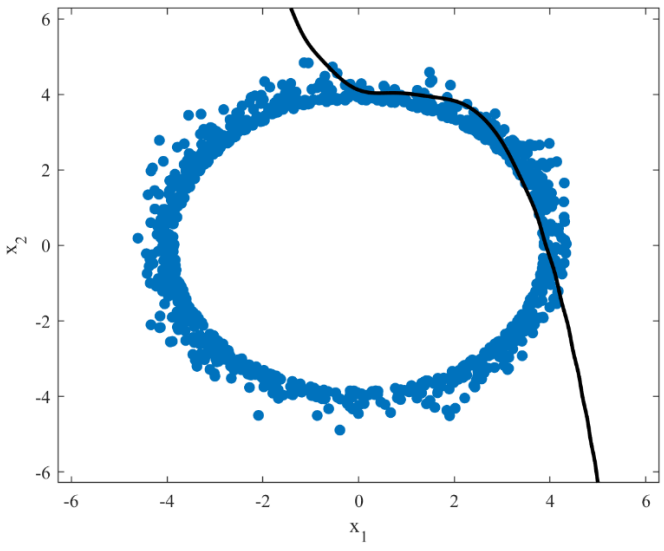

Fig. 4. The generated samples after truncating the JPDF in example 3

Example 4

This example has two standard normally distributed random variables, and its exponential LSF is as follows

$$g(X) = exp\big(0.2(1 + x_1 - x_2)\big) + exp\big(0.2(5 - 5x_1 - x_2)\big) - 1 \qquad (18)$$

The represented method has generated several samples in the failure domain and accurately computed the probability of failure by generating the required samples. Table 4 demonstrates that the proposed method achieves a more accurate estimation compared to MCS by generating the same number of samples. According to Table 4**,** by focusing sample generation on truncated JPDF, the probability of failure can be accurately estimated using sufficient samples. Fig. 5 indicates the generated samples using the truncated JPDF.

Table 4. Results of example 4

	Samples	Average N_f	STD N_f	Average P_f	Std P_f	P_f error (%)	CPU time
Proposed method	500	3.6	1.89	2.72×10^{-6}	1.28×10^{-6}	9.33	0.047
	1000	9.9	4.28	2.81×10^{-6}	5.90×10^{-7}	6.33	0.079
	5000	48.2	22.90	2.94×10^{-6}	4.24×10^{-7}	2.00	0.113
MCS	5000	0	0	0	0	100	0.119
FORM	-	-	-	7.89×10^{-6}	-	-	0.482
eKNN	5000	0	0	0	0	100	0.082

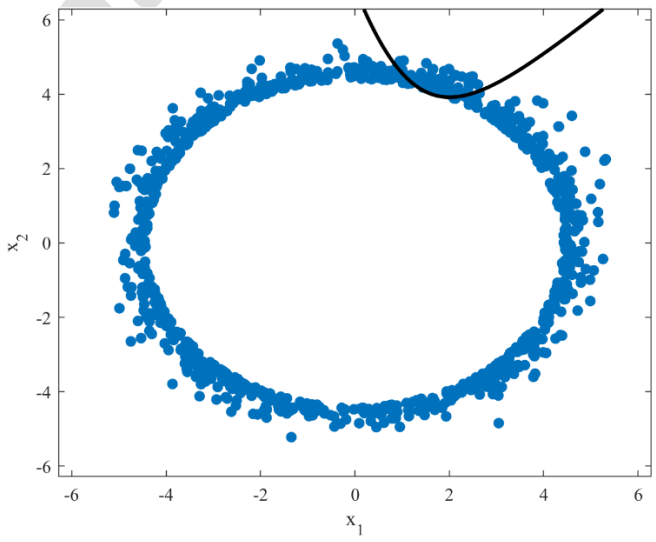

Fig. 5. The generated samples after truncating the JPDF in example 4

Example 5

In this example, the LSF is a bivariate polynomial as follows

$$g(X) = 150 + \frac{(x_1 + x_2)^2}{4} - 4(x_1 - x_2)^2 \tag{19}$$

The random variables have standard normal distributions. According to Table 5, while the MCS method fails to compute the failure probability, the proposed method estimates the P_f with high accuracy. Fig. 6 demonstrates the sample generation in the failure region, using the proposed method.

Table 5. Results of example 5

	Samples	Average N_f	STD N_f	Average P_f	Std P_f	P_f error (%)	CPU time
Proposed method	500	49	34.05	1.67×10^{-5}	1.75×10^{-6}	11.33	0.039
	1000	20	20.74	1.56×10^{-5}	4.55×10^{-6}	4.00	0.094
	5000	69	22.21	1.46×10^{-5}	1.76×10^{-6}	2.00	0.123
MCS	5000	0	0	0	0	100	0.125
FORM	-	-	-	NC	-	-	0.358
eKNN	5000	0	0	0	0	100	0.109

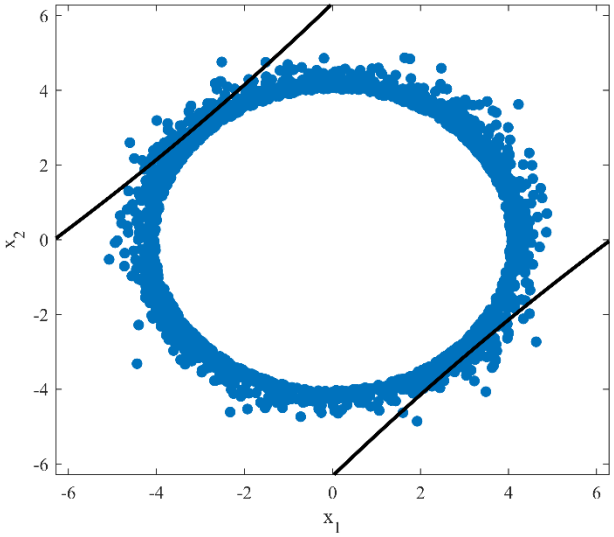

Fig. 6. The generated samples after truncating the JPDF in example 5

Example 6

In this example, the LSF is the following bivariate quartic polynomial

$$g(X) = x_1^4 + 2x_2^4 - 20 \quad (20)$$

x_1 and x_2 have normal distributions with means μ_1= μ_2=10 and standard deviations σ_1= σ_2= 5. In this example, the proposed method is able to evaluate the probability of failure without requiring many samples. The results in Table 6 show that by truncating the JPDF around the mean of the random variables, more samples are produced in the failure region, providing an estimation of failure probability with relatively high accuracy compared to the MCS method. The region of sample generation and the plot of the limit state surface are illustrated in Fig. 7.

Table 6. Results of example 6

	Samples	Average N_f	STD N_f	Average P_f	Std P_f	P_f error (%)	CPU time
Proposed method	500	7.1	2.18	0.0022	6.77×10^{-4}	15.78	0.032
	1000	13.3	2.83	0.0021	4.26×10^{-4}	10.52	0.067
	5000	46	7.83	0.0017	7.20×10^{-4}	10.52	0.112
MCS	5000	12	3.78	0.0025	7.56×10^{-4}	31.57	0.118
FORM	-	-	-	0.0092	-	-	0.304
eKNN	5000	11.5	1.65	0.0023	6.35×10^{-4}	21.05	0.113

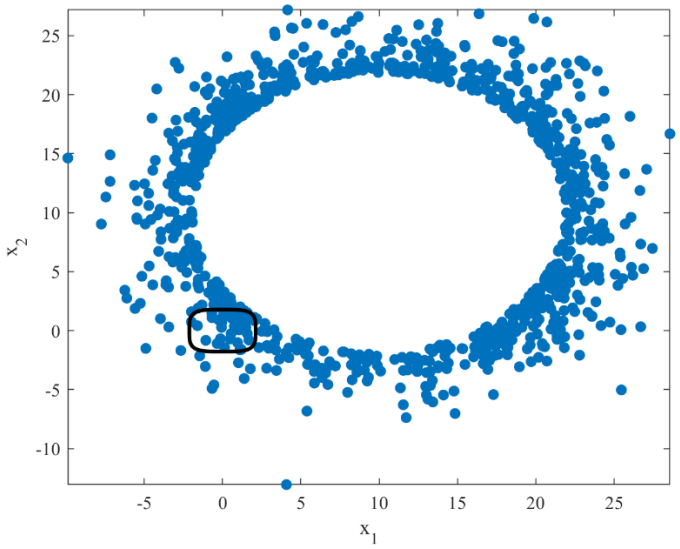

Fig. 7. The generated samples after truncating the JPDF in example 6

Example 7

This example is a conical structure, demonstrated in Fig. 8, containing a compressive axial load P and a bending moment M that are subjected to the structure.

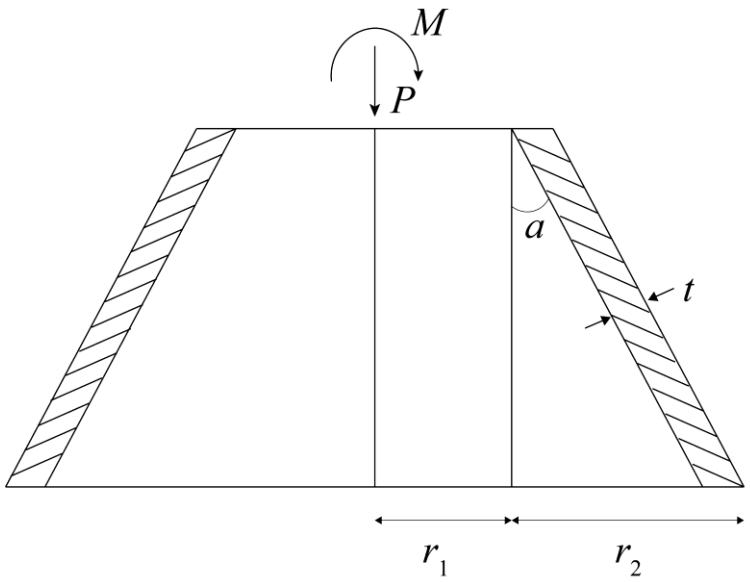

Fig. 8. The conical structure of example 7

The following equation determines the failure of this structure

$$\frac{P}{P_{cr}} + \frac{M}{M_{cr}} > 1 \tag{21}$$

where M_{cr} and P_{cr} are the critical bending moment and axial load, respectively, determined by

$$P_{cr} = \gamma \frac{2\pi E t^2 \cos^2 \alpha}{\sqrt{3(1-\nu^2)}} \tag{22}$$

$$M_{cr} = \eta \frac{2\pi E t^2 r_1 \cos^2 \alpha}{\sqrt{3(1-\nu^2)}} \tag{23}$$

To correlate the theoretical and experimental results, the coefficients γ and η (with values γ=0.33 and η=0.41) are applied. Conclusively, the following equation is indicated to define the LSF of this structure.

$$\mathrm{g}(\mathbf{X}) = 1 - \frac{\sqrt{3(1-\nu^2)}}{\pi E t^2 \cos^2 \alpha} \times \left(\frac{P}{2\gamma} + \frac{M}{\eta r_1}\right) \tag{24}$$

In which α is considered equal to 0.524. Table 7 illustrates the statistics of random variables.

Table 7. Statistics of random variables in example 7

Variable	Distribution	Mean	Standard deviation
E	Normal	70000	3500
t	Normal	2.5	0.125
r_1	Normal	900	22.5
M	Normal	8×10^7	6.4×10^6
P	Normal	70000	5600

By examining this example, it could be concluded that the computed probability of failure in the proposed method offers a more accurate estimation without requiring many samples. Table 8 provides the mentioned efficiency compared to MCS. As shown in the table, MCS fails to generate any sample in the failure region and cannot estimate the probability of failure.

Table 8. Results of example 7

	Samples	Average N_f	STD N_f	Average P_f	Std P_f	P_f error (%)	CPU time
Proposed method	1000	0.30	0.48	4.57×10^{-7}	8.57×10^{-7}	14.25	0.048
	5000	2	1.98	3.65×10^{-7}	3.17×10^{-7}	8.75	0.099
	10000	43	44.82	3.86×10^{-7}	9.68×10^{-8}	3.62	0.125
MCS	10000	0	0	0	0	100	0.136
FORM	-	0	0	8.07×10^{-7}	-	-	0.357
eKNN	10000	0	0	0	0	100	0.125

Example 8

In this example, a highly nonlinear LSF based on a two-degree-of-freedom primary-secondary dynamic system is presented, which is shown in Fig. 9. This example involves eight random variables: the masses m_p and m_s, spring stiffnesses k_p and k_s, damping ratios ξ_p and ξ_s, the force capacity of the secondary spring F_s, and finally the intensity of a white-noise base excitation of the system S_0, when p and s represent primary and secondary oscillators, respectively. The statistics of these eight random variables are summarized in Table 9.

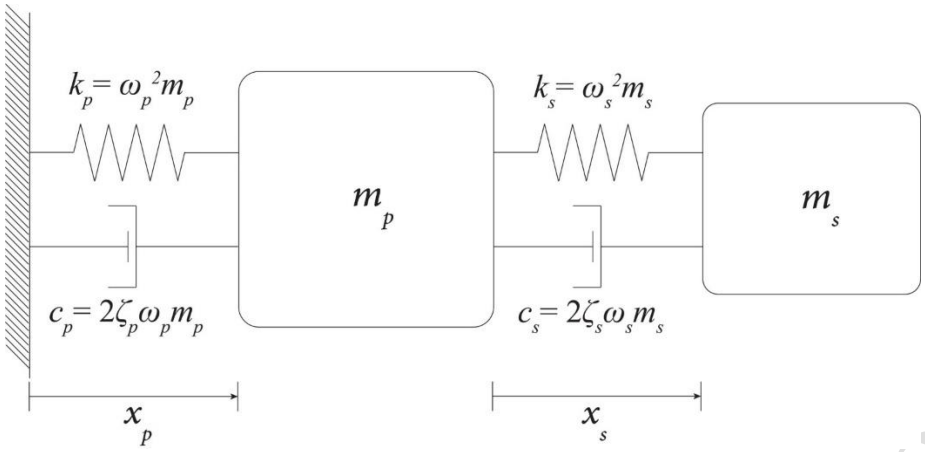

Fig. 9. Primary-secondary system of example 8

The LSF of this system is as follows

$$g = F_s - 3k_s p\sqrt{E} \tag{23}$$

$$E = \frac{\pi S_0}{4\zeta_s {\omega_s}^3}\left[\frac{\zeta_a \zeta_s}{\zeta_p \zeta_s\left(4{\zeta_a}^2 + \eta^2\right) + \nu {\zeta_a}^2}\frac{(\zeta_p {\omega_p}^3 + \zeta_s {\omega_s}^3)\omega_p}{4\zeta_a {\omega_p}^4}\right] \tag{24}$$

Table 9. Statistics of random variables in Example 8

Random Variables	Distribution	Mean	Standard Deviation
m_p	Normal	2	0.1
m_s	Normal	0.02	0.001
k_p	Normal	2	0.2
k_s	Normal	0.02	0.002
ξ_p	Normal	0.1	0.002
ξ_s	Normal	0.04	0.01
F_s	Normal	15	1.5
S_0	Normal	100	10

In these expressions, the natural frequencies of the primary and secondary oscillators are defined as $\omega_p = (k_p/m_p)^{0.5}$ and $\omega_s = (k_s/m_s)^{0.5}$. The average frequency and damping ratio are given by $\omega_a = (\omega_p + \omega_s)/2$ and $\xi_a = (\xi_p + \xi_s)/2$, respectively. The mass ratio is $\nu = m_s/m_p$, the tuning parameter is $\eta = (\omega_p - \omega_s)/\omega_a$, and the deterministic peak factor p is equal to 3.

Table 10. Results of example 8

	Samples	Average N_f	STD N_f	Average P_f	Std P_f	P_f error (%)	CPU time
	1000	15	3.27	8.00×10^{-4}	7.59×10^{-4}	27.27	0.038

Proposed method	5000	28	7.56	1.22×10^{-3}	4.41×10^{-4}	10.90	0.071
	10000	153	31.21	1.12×10^{-3}	1.32×10^{-4}	1.81	0.139
MCS	10000	9.5	3.69	9.50×10^{-4}	3.69×10^{-4}	13.64	0.141
FORM	-	-	-	NC	-	-	-
eKNN	10000	9	4.10	9.00×10^{-4}	6.89×10^{-4}	18.18	0.126

As shown in Table 10, the results indicate that the probability of failure derived by the proposed method offers a more accurate estimation compared to MCS. This improved accuracy is achieved without requiring a large number of samples, confirming the efficiency of the proposed method.

Example 9

In this example, a 25-bar spatial truss, illustrated in Fig. 10, is analyzed. The structure is subjected to seven concentrated loads applied at four different nodes. The directions of these loads are indicated in Fig. 10. The implicit LSF for this truss is expressed as follows

$$g = 2.5 - \Delta_A \qquad (25)$$

Where Δ_A denotes the displacement of node "A" in the Y-direction. The random variables and their statistics are summarized in Table 11. *A* represents the cross-sectional area of each section, and *E* is the modulus of elasticity of the members.

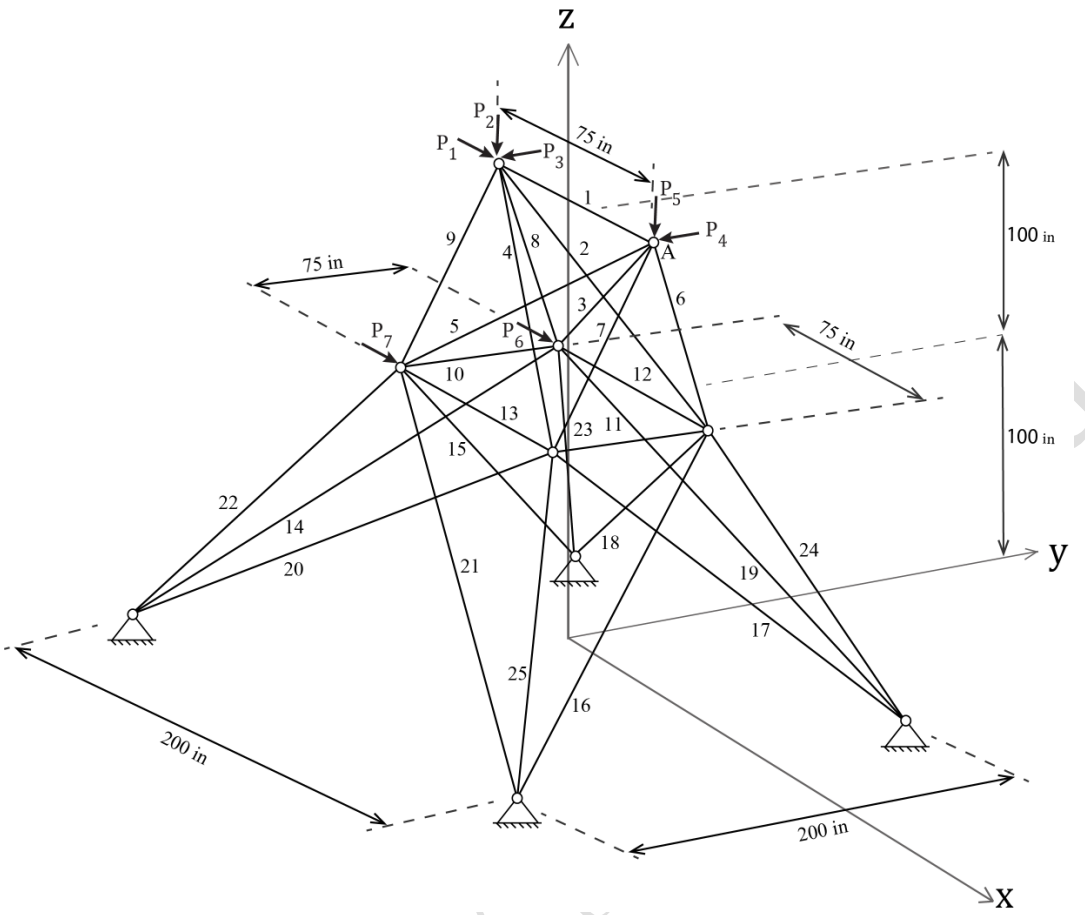

Fig. 10. The 25-bar spatial truss of example 9

Table 11. Statistics of random variables in example 9

Variables	Distribution	Mean	Standard deviation
P_1 (ksi)	Normal	1000	100
$P_{2\text{-}5}$ (ksi)	Normal	8000	800
$P_{6\text{-}7}$ (ksi)	Normal	1000	800
E (ksi)	Normal	2.04×10^6	2.04×10^5
A (in^2)	Normal	2	0.15

Based on the presented results, the proposed method is able to estimate the probability of failure with higher accuracy compared to the MCS, while requiring fewer samples. As shown in Table 12, the proposed method shows superior efficiency by concentrating on the effective regions and increasing the density of samples near the limit state surface. By truncating the JPDF around the mean of the random variables, more samples are generated in the failure region. This leads to a more accurate estimation of failure probability while reducing the number of required samples. Thus, the comparison indicates that the proposed method estimates the probability of failure more efficiently than the MCS approach.

Table 12. Results of example 9

	Samples	Average N_f	STD N_f	Average P_f	Std P_f	P_f error (%)	CPU time
Proposed method	1000	7	1.21	7.00×10^{-4}	9.10×10^{-5}	12.5	5.670
	5000	7.5	0.84	7.50×10^{-4}	6.12×10^{-5}	6.25	18.651
	10000	8.2	0.51	8.20×10^{-4}	3.98×10^{-5}	0.025	29.154
MCS	10000	14	2.65	6.00×10^{-4}	1.67×10^{-4}	25.00	30.104
FORM	-	-	-	NC	-	-	-
eKNN	10000	9.5	1.98	9.50×10^{-4}	1.25×10^{-4}	18.75	15.68

4. Conclusion

This study introduces a novel method to enhance the efficiency of Monte Carlo simulation for estimating the probability of failure in structural reliability analysis. Although Monte Carlo simulation is accurate, it often requires a large number of samples to achieve reliable results, leading to high computational costs. The proposed approach addresses these limitations by truncating the joint probability density function around the mean of random variables. First, a small number of uniformly distributed samples are generated, and the limit state function is evaluated at each sample. The radius of a circle that truncates the joint probability density function is defined as a specified percentage of the shortest distance from the mean to the samples in the failure region. Then, samples are generated within the outer area of the truncated region. In other words, the middle circular area centered at the mean is eliminated, and sample generation is more concentrated on the failure region. The volume under the truncated joint probability density function needs to be computed to determine the probability of failure. This volume is determinable using the regularized lower incomplete gamma function presented in the paper. Furthermore, the ability of the proposed method to enhance the efficacy is proven in several examples. In conclusion, the proposed method offers advancements in reliability analysis by providing a more efficient tool for estimating failure probability.

Acknowledgments

This research did not receive any specific grant from funding agencies in the public, commercial, or not-for-profit sectors.

References

Afshari, S. S., Enayatollahi, F., Xu, X. and Liang, X. (2022). "Machine learning-based methods in structural reliability analysis: A review", *Reliability Engineering & System Safety*, 219 108-223, https://doi.org/10.1016/j.ress.2021.108223.

Au, S.-K. and Beck, J. L. (2001). "Estimation of small failure probabilities in high dimensions by subset simulation", *Probabilistic Engineering Mechanics*, 16(4), 263-277, https://doi.org/10.1016/S0266-8920(01)00019-4.

Chen, G. and Yang, D. (2019). "Direct probability integral method for stochastic response analysis of static and dynamic structural systems", *Computer Methods in Applied Mechanics and Engineering*, 357 112-612, https://doi.org/10.1016/j.cma.2019.112612.

Chen, Z., Li, G., He, J., Yang, Z. and Wang, J. (2022). "Adaptive structural reliability analysis method based on confidence interval squeezing", *Reliability Engineering & System Safety*, 225 108639, https://doi.org/10.1016/j.ress.2022.108639.

Cheng, K. and Lu, Z. (2020). "Structural reliability analysis based on ensemble learning of surrogate models", *Structural Safety*, 83 101905, https://doi.org/10.1016/j.strusafe.2019.101905.

Cheng, Y., Zhuang, X. and Yu, T. (2024). "Time-dependent reliability analysis of planar mechanisms considering truncated random variables and joint clearances", *Probabilistic Engineering Mechanics*, 75 103-552, https://doi.org/10.1016/j.probengmech.2023.103552.

Dang, C., Valdebenito, M. A., Faes, M. G. R., Wei, P. and Beer, M. (2022). "Structural reliability analysis: A Bayesian perspective", *Structural Safety*, 99 102259, https://doi.org/10.1016/j.strusafe.2022.102259.

de Santana Gomes, W. J. (2019). "Structural Reliability Analysis Using Adaptive Artificial Neural Networks", *ASCE-ASME J Risk and Uncert in Engrg Sys Part B Mech Engrg*, 5(4), https://doi.org/10.1115/1.4044040.

Du, X. and hu, Z. (2012). "First Order Reliability Method With Truncated Random Variables", *Journal of Mechanical Design, Transactions of the ASME*, 134, https://doi.org/10.1115/1.4007150.

Guo, K., Yan, H., Huang, D. and Yan, X. (2022). "Active learning-based KNN-Monte Carlo simulation on the probabilistic fracture assessment of cracked structures", *International Journal of Fatigue*, 154 106-533, https://doi.org/10.1016/j.ijfatigue.2021.106533.

Hao, P., Yang, H., Yang, H., Zhang, Y., Wang, Y. and Wang, B. (2022). "A sequential single-loop reliability optimization and confidence analysis method", *Computer Methods in Applied Mechanics and Engineering*, 399 115400, https://doi.org/10.1016/j.cma.2022.115400.

Hasofer, A. M. and Lind, N. C. (1974). "Exact and invariant second-moment code format", *Journal of the Engineering Mechanics division*, 100(1), 111-121, https://doi.org/10.1061/JMCEA3.0001848.

Hong, L., Li, H., Gao, N., Fu, J. and Peng, K. (2021). "Random and multi-super-ellipsoidal variables hybrid reliability analysis based on a novel active learning Kriging model", *Computer Methods in Applied Mechanics and Engineering*, 373 113555, https://doi.org/10.1016/j.cma.2020.113555.

Jafari-Asl, J., Ben Seghier, M. E. A., Ohadi, S., Correia, J. and Barroso, J. (2022). "Reliability analysis based improved directional simulation using Harris Hawks optimization algorithm for engineering systems", *Engineering Failure Analysis*, 135 106148, https://doi.org/10.1016/j.engfailanal.2022.106148.

Kamiński, M. and Solecka, M. (2013). "Optimization of the truss-type structures using the generalized perturbation-based Stochastic Finite Element Method", *Finite Elements in Analysis and Design*, 63 69-79, https://doi.org/10.1016/j.finel.2012.08.002.

Keshtegar, B. and Kisi, O. (2017). "M5 model tree and Monte Carlo simulation for efficient structural reliability analysis", *Applied Mathematical Modelling*, 48 899-910, https://doi.org/10.1016/j.apm.2017.02.047.

Keshtegar, B. and Miri, M. (2013). "An enhanced HL-RF method for the computation of structural failure probability based on relaxed approach", *Civil Engineering Infrastructures Journal*, 46(1), 69-80, https://doi.org/10.7508/ceij.2013.01.005.

Kumar, A., Rai, B. and Samui, P. (2024). "Hybrid neuro-fuzzy ML and MC simulation-based Reliability Analysis of Simply Supported Beam", *Civil Engineering Infrastructures Journal*, https://doi.org/10.22059/ceij.2024.374883.2045.

Lu, P., Hong, T., Wu, Y., Xu, Z., Li, D., Ma, Y. and Shao, L. (2022). "Kriging–KNN Hybrid Analysis Method for Structural Reliability Analysis", *Journal of Bridge Engineering*, 27(4), 04022009, https://doi.org/10.1061/(ASCE)BE.1943-5592.000183.

Luo, C., Keshtegar, B., Zhu, S. P., Taylan, O. and Niu, X.-P. (2022). "Hybrid enhanced Monte Carlo simulation coupled with advanced machine learning approach for accurate and efficient structural reliability analysis", *Computer Methods in Applied Mechanics and Engineering*, 388 114218, https://doi.org/10.1016/j.cma.2021.114218.

Meng, D., Yang, H., Yang, S., Zhang, Y., De Jesus, A. M., Correia, J., Fazeres-Ferradosa, T., Macek, W., Branco, R. and Zhu, S.-P. (2024a). "Kriging-assisted hybrid reliability design and optimization of offshore wind turbine support structure based on a portfolio allocation strategy", *Ocean Engineering*, 295 116842, https://doi.org/10.1016/j.oceaneng.2024.116842.

Meng, D., Yang, S., De Jesus, A. M., Fazeres-Ferradosa, T. and Zhu, S.-P. (2023a). "A novel hybrid adaptive Kriging and water cycle algorithm for reliability-based design and optimization strategy: Application in offshore wind turbine monopile", *Computer Methods in Applied Mechanics and Engineering*, 412 116083, https://doi.org/10.1016/j.cma.2023.116083.

Meng, D., Yang, S., De Jesus, A. M. and Zhu, S.-P. (2023b). "A novel Kriging-model-assisted reliability-based multidisciplinary design optimization strategy and its application in the offshore wind turbine tower", *Renewable Energy*, 203 407-420, https://doi.org/10.1016/j.renene.2022.12.062.

Meng, D., Yang, S., Yang, H., De Jesus, A. M., Correia, J. and Zhu, S.-P. (2024b). "Intelligent-inspired framework for fatigue reliability evaluation of offshore wind turbine support structures under hybrid uncertainty", *Ocean Engineering*, 307 118-213, https://doi.org/10.1016/j.oceaneng.2024.118213.

Peng, X., Li, D.-Q., Cao, Z.-J., Gong, W. and Juang, C. H. (2017a). "Reliability-based robust geotechnical design using Monte Carlo simulation", *Bulletin of Engineering Geology and the Environment*, 76(3), 1217-1227, https://doi.org/10.1007/s10064-016-0905-3.

Peng, X., Li, D.-Q., Cao, Z.-J., Gong, W. and Juang, C. H. (2017b). "Reliability-based robust geotechnical design using Monte Carlo simulation", *Bulletin of Engineering Geology and the Environment*, 76 1217-1227, https://doi.org/10.1007/s10064-016-0905-3.

Pokusiński, B. and Kamiński, M. (2023). "Numerical convergence and error analysis for the truncated iterative generalized stochastic perturbation-based finite element method", *Computer Methods in Applied Mechanics and Engineering*, 410 115993, https://doi.org/10.1016/j.cma.2023.115993.

Qin, Q., Cao, X. and Zhang, S. (2022). "AWK-TIS: An Improved AK-IS Based on Whale Optimization Algorithm and Truncated Importance Sampling for Reliability Analysis", *CMES - Computer Modeling in Engineering and Sciences*, 135(2), 1457-1480, https://doi.org/10.32604/cmes.2023.022078.

Roudak, M. A., Farahani, M. and Hosseinbeigi, F. B. (2024). "Extension of K-nearest neighbors and introduction of an applicable prediction criterion for a novel Monte Carlo simulation-based method in structural reliability", *Structures*, 66 106867, https://doi.org/10.1016/j.istruc.2024.106867.

Roudak, M. A., Karamloo, M., Shayanfar, M. A. and Ardalan, R. (2023) "A non-gradient-based reliability method using a new six-item instruction for updating design point", *Structures*, Elsevier, 1752-1766, https://doi.org/10.1016/j.istruc.2023.03.012.

Roy, A. and Chakraborty, S. (2023). "Support vector machine in structural reliability analysis: A review", *Reliability Engineering & System Safety*, 233 109126, https://doi.org/10.1016/j.ress.2023.109126.

Shayanfar, M. A., Barkhordari, M. A. and Roudak, M. A. (2018). "A Modification to HL-RF Method for Computation of Structural Reliability Index in Problems with Skew-distributed Variables", *KSCE Journal of Civil Engineering*, 22(8), 2899-2905, https://doi.org/10.1007/s12205-017-1473-1.

Sun, H., Burton, H. V. and Huang, H. (2021). "Machine learning applications for building structural design and performance assessment: State-of-the-art review", *Journal of Building Engineering*, 33 101-816, https://doi.org/10.1016/j.jobe.2020.101816.

Wang, Q., Li, Q., Wu, D., Yu, Y., Tin-Loi, F., Ma, J. and Gao, W. (2020). "Machine learning aided static structural reliability analysis for functionally graded frame structures", *Applied Mathematical Modelling*, 78 792-815, https://doi.org/10.1016/j.apm.2019.10.007.

Xiao, N.-C., Duan, L. and Tang, Z. (2017). "Surrogate-model-based reliability method for structural systems with dependent truncated random variables", *Proceedings of the Institution of Mechanical Engineers, Part O: Journal of Risk and Reliability*, 231(3), 265-274, https://doi.org/10.1177/1748006X17698065.

Xiao, N.-C., Yuan, K. and Zhou, C. (2020). "Adaptive kriging-based efficient reliability method for structural systems with multiple failure modes and mixed variables", *Computer Methods in Applied Mechanics and Engineering*, 359 112649, https://doi.org/10.1016/j.cma.2019.112649.

Xiao, X., Li, Q. and Wang, Z. (2023). "A robust method for reliability updating with equality information using sequential adaptive importance sampling", *Computer Methods in Applied Mechanics and Engineering*, 410 116028, https://doi.org/10.1016/j.cma.2023.116028.

Yang, D. (2010). "Chaos control for numerical instability of first order reliability method", *Communications in Nonlinear Science and Numerical Simulation*, 15(10), 3131-3141, https://doi.org/10.1016/j.cnsns.2009.10.018.

Yang, S., Meng, D., Yang, H., Luo, C. and Su, X. (2025) "Enhanced soft Monte Carlo simulation coupled with support vector regression for structural reliability analysis", *Proceedings of the Institution of Civil Engineers-Transport*, Emerald Publishing Limited, 1-16, https://doi.org/10.1680/jtran.24.00128.

Yeh, W.-C. (2022). "Novel self-adaptive Monte Carlo simulation based on binary-addition-tree algorithm for binary-state network reliability approximation", *Reliability Engineering & System Safety*, 228 108796, https://doi.org/10.1016/j.ress.2022.108796.

Zhang, Y. and Xu, J. (2021a). "Efficient reliability analysis with a CDA-based dimension-reduction model and polynomial chaos expansion", *Computer Methods in Applied Mechanics and Engineering*, 373 113-467, https://doi.org/10.1016/j.cma.2020.113467.

Zhang, Y. and Xu, J. (2021b). "Efficient reliability analysis with a CDA-based dimension-reduction model and polynomial chaos expansion", *Computer Methods in Applied Mechanics and Engineering*, 373 113-467, https://doi.org/10.1016/j.cma.2020.113467.

Zhou, T., Guo, T., Dong, Y. and Peng, Y. (2024). "Structural reliability analysis based on probability density evolution method and stepwise truncated variance reduction", *Probabilistic Engineering Mechanics*, 75 103580, https://doi.org/10.1016/j.probengmech.2024.103580.

Zhou, Y., Lu, Z. and Yun, W. (2020). "Active sparse polynomial chaos expansion for system reliability analysis", *Reliability Engineering & System Safety*, 202 107025, https://doi.org/10.1016/j.ress.2020.107025.

Zhu, S.-P., Keshtegar, B., Chakraborty, S. and Trung, N.-T. (2020). "Novel probabilistic model for searching most probable point in structural reliability analysis", *Computer Methods in Applied Mechanics and Engineering*, 366 113027, https://doi.org/10.1016/j.cma.2020.113027.